

Electronic structure of highly ordered films of self-assembled graphitic nanocolumns

R. Friedlein,^{1,*} X. Crispin,¹ C. D. Simpson,² M. D. Watson,^{2,†} F. Jäkel,³ W. Osikowicz,¹ S. Marciniak,¹ M. P. de Jong,¹ P. Samori,^{3,‡} S. K. M. Jönsson,^{1,4} M. Fahlman,^{1,4} K. Müllen,² J. P. Rabe,³ and W. R. Salaneck¹

¹Department of Physics (IFM), Linköping University, 581 83 Linköping, Sweden

²Max Planck Institute for Polymer Research, Ackermannweg 10, 55128 Mainz, Germany

³Department of Physics, Humboldt University Berlin, Newtonstrasse 15, 12489 Berlin, Germany

⁴Department of Science and Technology, ITN, Linköping University, 601 74 Norrköping, Sweden

(Received 24 May 2003; revised manuscript received 12 August 2003; published 20 November 2003)

Highly ordered, several nanometers thick films of alkylated large planar, polycyclic aromatic hydrocarbon (PAH) molecules have been grown on semi-metallic molybdenum disulfide substrates. The films are characterized by a two-dimensional lateral arrangement of columns standing at the surface on a macroscopic scale. The self-assembly of such insulated columns of face-to-face disks with surface-induced vertical alignment has been achieved directly from solution processing. Angle-resolved photoelectron spectra revealed a highly anisotropic quasi-one-dimensional electronic structure with an extended π -electronic wave function. An intermolecular dispersion of the highest occupied band of at least 0.15 eV along the stacking direction has been measured. A partial breakdown of the concept of quasimomentum due to the finite size of the nano-objects perpendicular to the stacks is observed.

DOI: 10.1103/PhysRevB.68.195414

PACS number(s): 73.22.Dj, 61.30.Hn, 64.70.Md, 79.60.Fr

I. INTRODUCTION

Self-assembled, nanostructured films of polycyclic aromatic hydrocarbons (PAH's) with unique electronic^{1,2} and opto-electronic³ properties can be designed by tuning the size and shape of the aromatic core and of the attached side chains. The latter allow solution processing which, in the framework of organic-electronics applications, has great advantages due to low manufacturing costs and process simplicity. Control of molecular order is critical for optimizing the performance of organic electronic devices such as organic field-effect transistors (OFET's),⁴ sensors,^{5,6} and solar cells.³ Photovoltaic devices based on spin-coated blends of phase segregated organic crystal networks have reached high external quantum efficiencies.³ Within the individual phases, an efficient transport of charges away from the exciton dissociation site was achieved due to stacking of the molecules in self-assembled liquid-crystalline (LC) and crystalline structures. In the LC phase, discotic columnar structures of substituted hexa-*peri*-hexabenzocoronenes (HBC's) possess coaxially insulated, conductive pathways, with a coherence length approaching 500 nm.⁷ Even in nonoptimally processed HBC materials, the sum of all intracolumnar charge mobilities reaches up to about $0.4 \text{ cm}^2 \text{ V}^{-1} \text{ s}^{-1}$.^{1,2} These columns are true nanostructures, with a diameter of about 1 nm given by the size of the aromatic HBC core which contains 42 carbon atoms. Their quasi-one-dimensional nature should allow the exploration of novel effects related to quantization in the directions perpendicular to the main columnar axis. Furthermore, in the stacking direction, these columns have electronic properties that resemble graphite, with π molecular orbitals originating from the overlap of the atomic p_z orbitals oriented parallel to the column axis. In this regard, the HBC stacks can be seen as "quasi-one-dimensional graphite," complementary to carbon nanotubes where the π orbitals are perpendicular to the axis.⁸

Alkylated HBC's have been previously self-assembled

from solution into highly ordered architectures on a surface.^{9–11} Dry monolayers of HBC- C_{12} (compound 1b shown in Fig. 1) could be physisorbed on the [0001] plane of highly oriented pyrolytic graphite (HOPG). The disk like molecules were found to lie flat on the substrate surface, assembled into supramolecular anisotropic structures oriented in preferential directions according to the threefold symmetry of the substrate.¹¹ In contrast, for thicker films processed from solutions with a higher molecular concentration, a lower degree of azimuthal order was obtained.¹¹ Under proper solution processing conditions employing temperature/concentration gradients, it is possible to produce thin films with near perfect alignment of columns parallel to the substrate, as is optimal for OFET performance.⁷

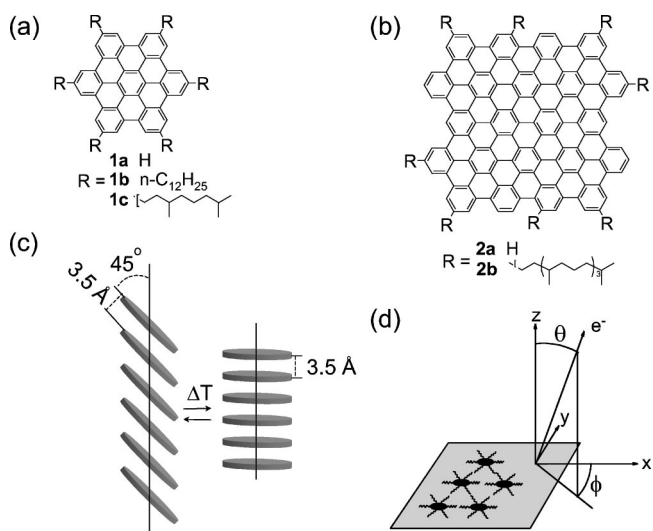


FIG. 1. Chemical structure of (a) HBC's and (b) derivatives of C_{132} . (c) Schematic illustration of typical thermotropic behavior of substituted derivatives of discotic PAH's. (d) The geometry of the photoelectron emission experiments.

It is also desirable to prepare films with columns perpendicular to surfaces (homeotropic). Such films of standing graphitic nanocolumns might serve as field emitters utilizing a high electric-field strength at the tip of the columns such as in carbon nanotube field-emission displays.¹² In the case of photovoltaic devices conducting columnar pathways could connect parallel large-area transparent electrodes. The importance of alignment in this geometry has been made clear, where short-circuit photoconductivities of thin films of an alkylated HBC sandwiched between two indium-tin oxide electrodes is about five times increased in areas with good homeotropic alignment.¹³ It was recently shown for a variety of columnar phase-forming materials that this alignment is in fact thermodynamically favored, but can be achieved at a single surface (not sandwich) only after cooling sufficiently thin films from the melt.¹⁴ Vertically stacked columns of unsubstituted HBC (1a), a few molecules in height, can also be grown by ultrahigh vacuum (UHV) vapor deposition,¹⁵ utilizing a first-formed face-on monolayer as the ground floor. Given the sometimes practically inaccessible high temperatures needed for isotropization or sublimation of columnar discotics, it is important to address whether substrate-induced order characterized by columns oriented normal to the substrate can be achieved upon the complementary solution processing.

In this paper, we report on the solution processing of 2–6-nm-thick films of alkylated PAH molecules exhibiting homeotropically ordered architectures at a flat, semimetallic substrate surface and the determination of their electronic structure by photoelectron spectroscopy. Two PAH's of different size and shape, namely, hexa(3,7-dimethyloctanyl)hexa-*peri*-hexabenzocoronene, or HBC-C_{8,2} (1c), and C₁₃₂-C_{16,4} (2b) (Fig. 1) are chosen. Other derivatives of HBC and C₁₃₂ would be difficult or impossible to align thermally due their high isotropization temperatures ($\sim 400^\circ\text{C}$ and $>600^\circ\text{C}$, respectively), and may not be sublimed cleanly due to thermally labile side chains. Although monolayers and doublelayers of 1a and 2a have been formed by solution processing,⁹ thicker films are unlikely to be achieved due to the vanishing solubility of the molecules. Both 1c and 2b studied here carry racemic-branched side chains which grant good solubility in organic solvents.

II. EXPERIMENT

A. Film preparation

The synthesis of 1c was carried out as published;¹⁶ that of 2b will be published separately.¹⁷ The molecules were dissolved in boiling *p* xylene, in a concentration of 0.02 g/l. The solutions, kept at about 70°C (for HBC-C_{8,2}) or 90°C (for C₁₃₂-C_{16,4}), were then deposited onto freshly cleaved MoS₂ [0001] substrates (JEOL, B. V. Belgium), which were held at the same temperatures, in order to prevent precipitation. To minimize kinetic trapping of columns randomly oriented relative to the surface during solvent evaporation, the drying process was slowed (~ 10 min) by performing the processing in an almost saturated atmosphere of the solvent. By choosing the particular solvent *p* xylene and suitable prepa-

ration temperatures a subtle balance between a sufficient solubility and a suitable evaporation rate of the solvent was attained.

As-prepared samples were introduced to the UHV system of the spectrometer and annealed at temperatures between 90°C and 140°C , over successive 10-min intervals, each followed by spectroscopic characterization as described below. For each heating period, the temperature was increased by 10°C in order to detect possible phase transitions and the temperatures at which they occur. In the thin films of 1c, a distinct irreversible change in the spectra occurred between 80°C and 90°C . That is, upon cooling to room temperature, the spectral features did not revert to those of the as-prepared film. For 2b, annealing at about 130°C made an even more significant change in terms of the intensity of the relevant features.

As a reference system for the alkylated PAH's, highly ordered films of HBC (1a) molecules, similar to films already characterized,¹⁸ were prepared by vapor deposition in UHV onto similar MoS₂ [0001] substrates.

B. Spectroscopy and microscopy

Angle-resolved ultraviolet photoelectron spectroscopy (ARUPS) was carried out using polarized synchrotron radiation from the MAX-II storage ring of the MAX Laboratory for Synchrotron Radiation Facility in Lund, Sweden. Spectra were taken with the angle-resolving photoelectron spectrometer at the beam line I411, using 60-eV photons. The background pressure in the end station was lower than 8×10^{-10} mbars. A detailed description of the beam line I411 and its end station is given elsewhere.¹⁹ The experimental geometry is sketched in Fig. 1(c). The electron energy analyzer and the sample are rotatable around the axis of the incident light, which limits the available photoelectron emission angle θ to the range between 15° and 90° . The angle between the electric-field vector of the incident light and the sample surface normal is fixed to 15° . An angular resolution of about 5° and an energy resolution of about 100 meV was employed. The spatial resolution was on the order of 1 mm^2 . The spectra are normalized to the incoming photon flux. They are plotted on a binding-energy scale relative to the Fermi level (E_F) of the spectrometer, as determined from a sputtered and annealed gold substrate prior to the measurements for a set of polar photoelectron emission angles θ , as defined with respect to the substrate surface normal. No radiation damage of the samples was observed since the shape and energy of valence-band spectral features were unchanged even after a few hours of irradiation.

The work function of similarly prepared films was measured from the cutoff of the secondary electrons²⁰ in HeI spectra employing a home-built photoelectron spectrometer. For the determination of the ionization potential (IP), the work function was added to the onset of the spectral weight at low binding energies as measured with respect to E_F . In order to determine the nominal film thickness from the suppression of the substrate core-level lines, measured by x-ray photoelectron spectroscopy, molybdenum disulfide was chosen as substrate instead of HOPG that has been employed in

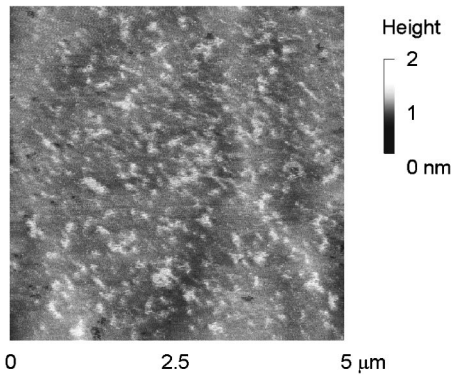


FIG. 2. Topographical TM-SFM image of an annealed multilayer 1c film.

previous works.^{9,11} The nominal thickness of the 1c and 2b films was estimated to be between 3 ± 2 and 6 ± 2 nm by applying tabulated values for the inelastic mean free path obtained for materials containing aromatic rings.²¹

The morphology of 1c pristine films is studied in air by tapping-mode scanning force microscopy (TM-SFM) in a Nanoscope IIIa system (Digital Instruments, Santa Barbara, CA). Both the height and the phase signal have been recorded with a scan rate of 0.2 lines/s and a lateral resolution of 512 pixels. Surface profiles were quantified using the NANOSCOPE software. Noncontact “golden” silicon cantilevers (NT-MDT, Russia) with a tip height of 10–20 μm and a typical curvature radius of less than 10 nm were used.

III. RESULTS AND DISCUSSION

A. HBC- $C_{8,2}$

Figure 2 displays a TM-SFM image of an annealed 1c film. The film is flat within 1–2 nm, over several μm^2 large areas. This is different from 1b films produced by fast solution processing on HOPG [0001] (Ref. 11) which are not ordered on a macroscopic scale. Since the nominal thickness is 3 to 6 nm (between 10 and 20 layers), we conclude that the substrate is completely covered. Very small grains can be recognized on the top of the film probably resulting from fast solvent evaporation in the final stage of film preparation.

Figure 3(a) shows valence-band photoelectron spectra recorded on as-prepared (dotted line) and annealed (full circles, full line) 1c films. The latter were kept at 140 °C during the time of the measurements (subsequent spectra measured at room temperature are identical). Figure 3(b) shows parts of the spectra on an expanded scale. Features at binding energies up to 4 eV are predominantly due to π -electronic states. They appear at small angles with a remarkably high intensity up to $\theta \approx 35$ –40 deg, above which they decrease with increasing θ . Films produced with non-optimal processing gave spectral features of significantly diminished intensity, and no angular dependence. Individual features at low binding energy are recognizable at 1.15 (IP = 5.5 eV, labeled A), 1.70 (labeled C), 2.55 (labeled D), 3.65 and 4.10 eV, and as a shoulder at 1.40 eV (labeled B). Features A, B, and C, which contribute to a broader feature in the spectra of 1b monolayer films,⁹ correspond to the three

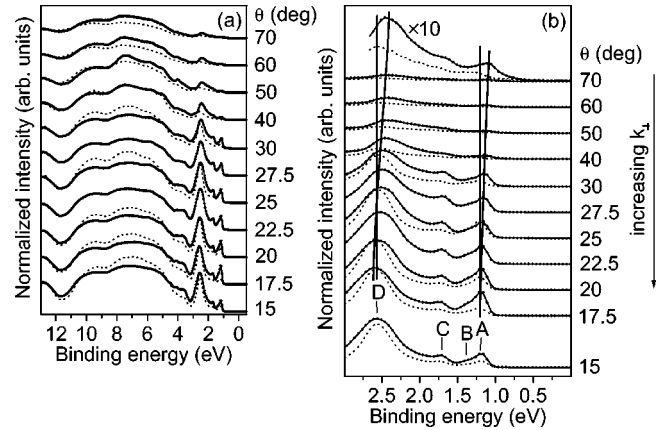


FIG. 3. ARUPS spectra of annealed (full line, circles) and as-prepared (dotted line) HBC- $C_{8,2}$ (1c) films in a wider (a) and narrower (b) energy range. Additionally, the shift of peaks A and D with the polar photoelectron emission angle θ in the annealed films is indicated by a thick full line. Peaks in the spectra of the as-prepared films do not disperse. Uppermost spectrum in (b): that of the annealed film at $\theta = 70$ deg magnified by a factor of 10.

least-bound states in HBC.²² A high density of states leading to the relatively broad and intense feature D centered at 2.55 eV is very similar to the one observed for graphite and carbon nanotubes,⁸ where it corresponds to states at the M point of the hexagonal Brillouin zone of the graphene lattice.^{23,24} As for other aromatic systems, including graphite,^{8,23,25} features in the binding-energy region between 4 and 8 eV correspond to a mixture of states of π and σ symmetry,¹⁸ which also appear at higher emission angles.

Figure 4 shows the angular distribution of the photoelectron intensity (peak height) of distinct features of the 1c films, namely, peak A, which is derived from the highest occupied molecular orbital (HOMO), and of peak D. The intensity of A is high in a narrow angle range, between about $15 \text{ deg} < \theta < 35 \text{ deg}$, whereas D is intense in a wider range, from below $\theta = 15$ deg to high angles with decreasing intensities in the tail. The pronounced angular dependence of the photoelectron intensity in both cases indicates a high degree

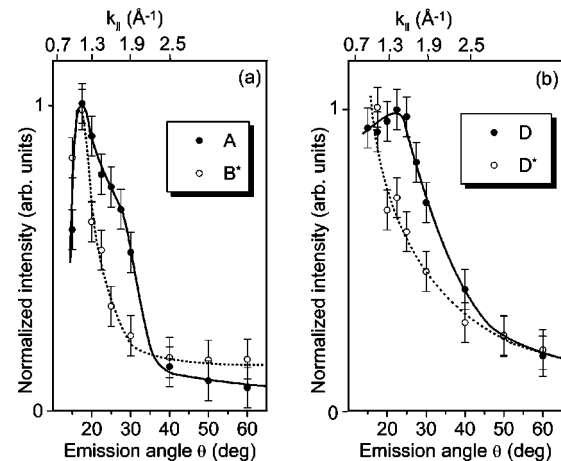


FIG. 4. Angular distribution of the photoelectron intensity of (a) peaks A and B^* and (b) peaks D and D^* .

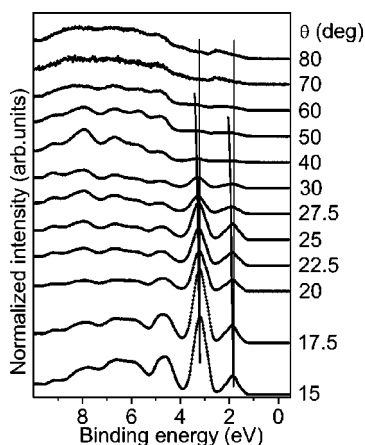


FIG. 5. ARUPS spectra of ordered HBC (1a) films prepared by vapor deposition on a MoS₂ [0001] surface, as a function of the polar photoelectron emission angle θ .

of molecular order in the surface region of the films.^{26,27} Differences between the pattern for *A* and *D* indicate an orbital dependence of the emission. For another type of disk-like aromatic molecules, phthalocyanines, photoelectrons from π orbitals are emitted essentially in a cone symmetrical around the normal of the molecular plane, with the highest intensity at angles other than zero.²⁸ Its exact shape depends on the particular orbital, the photon energy, and the direction of the electric-field vector with respect to the orientation of the molecule.²⁹ For the flat PAHs, the emission pattern is expected to be related to the graphene-derived nature and the finite size of the molecules, as proposed further below.

The photoelectron emission pattern in Fig. 3(a) resembles that of ~ 20 -nm-thick highly ordered films of 1a molecules sublimed on MoS₂ substrates, as displayed in Fig. 5. Such relatively thick HBC films consist of tightly packed, atomically flat domains with a diameter between 100 and 700 nm.¹⁸ On single islands, monomolecular steps with heights of 3.3–3.6 Å have been observed, in good agreement¹⁸ with the interplanar distance (3.42 Å) between molecules in a HBC single crystal.³⁰ The HBC molecules most likely form supramolecular columns with the axis oriented normal to the substrate surface such as in HBC films on Cu [111] and Au [111] surfaces.¹⁵ The similarity in the photoelectron angular pattern between the HBC (1a) and the solution processed HBC-C_{8,2} (1c) films suggests therefore a *molecular orientation parallel to the substrate* for both the as-prepared and heated 1c films.³¹

The polar angular dependence of the photoelectron emission can now be discussed in more detail. The momentum of the photoelectron corresponds to the initial-state wave vector of the electron inside the solid.³² The in-plane components k_x and k_y are preserved, and can be derived from the polar, θ , and azimuthal, ϕ , electron emission angles. For layered systems, k_x and k_y have a meaning in terms of the two-dimensional band structure of the individual layers. For layered films of HBC molecules, on the macroscopic scale probed by the photon beam, all the individual molecules do not have the same single in-plane orientation. This is because of the rotational degree of freedom around the z axis,⁹ de-

fining as normal to the substrate surface. Therefore it is reasonable to plot, and to discuss, the spectra in terms of an in-plane wave number $k_{\parallel} = (k_x^2 + k_y^2)^{1/2} \propto \sin(\theta)$. For photoelectrons with a kinetic energy of about 54 eV, photoionized by 60-eV photons, the angle $\theta \approx 25.4$ deg corresponds to a wave number of the escaping electron similar to that of the size of the Brillouin zone of graphene which is about 1.63 \AA^{-1} . The observation of emission at higher angles cannot be attributed to the angular resolution of the spectrometer alone (5 deg), but additionally suggests initial-state smearing of k_x and k_y , and thereby k_{\parallel} , by about $\Delta k \sim 0.55 \text{ \AA}^{-1}$ (i.e., $\Delta \theta \approx 10$ deg), due to the restriction of the electronic wave function over the finite size of the molecular core (about 11 Å). That is, k_x and k_y of the individual electronic states do not correspond exactly to those expected for a wave function in an infinitely extended graphene lattice. This phenomenon is discussed in detail for films of *p*-sexiphenyl molecules,³³ a system which represents a one-dimensional counterpart of the quasi-two-dimensional electronic system of the nanographenes. In this regard, the electron emission pattern reflects the graphenelike nature as well as the finite size of the molecules and their supramolecular nanostructures.

Figure 3(b) shows a close-up of the low-binding-energy regions of the HBC-C_{8,2} spectra of Fig. 3(a). Subtle but important differences in the electronic structure of the two systems are revealed. Only for films after heating to 80–90 °C, a clear shift of all peaks towards lower binding energy with increasing θ is observed. Since in both films molecular cores are oriented flat with respect to the substrate surface normal, this shift is not related to an in-plane “quasidispersion” which is reflected in an observable different angular emission pattern for the features *A* and *D* (Fig. 4). Rather, the shift in the annealed films is attributed to a dispersion of electronic states along columns of HBC-C_{8,2} molecules, that is, with respect to the wave vector $k_{\perp} = k_z$. This band formation is related to a *columnar arrangement with the axis perpendicular to the substrate surface and a significant intermolecular π - π overlap*. Note that the observation of peak shifts towards higher binding energies with θ in the spectra of 1a films might indicate a band dispersion as well. Such a conclusion, however, is not straightforward since the corresponding ordered reference system (without an intermolecular band dispersion) does not exist.

The k_{\perp} component of the photoelectron momentum is not preserved when passing through the film-vacuum interface.³² For this reason it is unclear whether or not in the annealed films the dispersion within one of the higher Brillouin zones is complete in the spectrum between angles of $\theta = 15$ deg and 70 deg. However, for the least bound states, derived from the HOMO, a peak shift of about 0.15 ± 0.05 eV is observed. This might serve as a lower estimate of the HOMO electronic one-particle bandwidth W . Since the shape of the peak does not essentially change with θ , the observed dispersion might even correspond to that of each single vibrational substate. A value of W of about 0.1–0.2 eV is of the same order of magnitude as those observed for the only other, to our best knowledge, single-component organic systems, namely, bis(1,2,5-thiadiazolo)-*p*-quinobis(1,3-dithiole),³⁴ where dispersing bands could be observed in the bulk of the solid. The

observed value is, however, substantially smaller than that of graphite which is about 1 eV.²⁴ For thin annealed films of 1c the observed intermolecular band dispersion indicates, first, that columnar stacks are indeed formed on a macroscopic scale and, second, that within these columns *the electronic wave function is highly extended in the stacking direction*. Clearly, highly oriented quasi-one-dimensional stacks of molecules represent one of the best systems for basic studies of the formation of extended electronic states in molecular solids. A large electronic intermolecular π - π overlap of up to 1 eV was predicted to occur for discotic liquid crystals of substituted triphenylene³⁵ and HBC,³⁶ which is thought to be responsible for the anisotropic, high mobilities^{1,2} observed for a number of discotic mesogens of aromatic hydrocarbons. At finite temperatures, W is significantly reduced due to geometric fluctuations, which involve intramolecular as well as rotational and translational degrees of freedom of the individual molecules.³⁵

The phase behavior within these ultrathin films is dramatically different from that observed in the bulk. Below its isotropization temperature ($\sim 400^\circ\text{C}$) 1c undergoes a single reversible thermal transition at $\sim 80^\circ\text{C}$.¹⁶ In the bulk, the disk planes are tilted by 40–50 deg relative to the columnar axes below this temperature,³⁷ and perpendicular to the columnar axis above, as depicted in Fig. 1(a). It is a common feature of π systems stacked in a face-to-face manner to maintain a lateral offset to optimize orbital interactions, which is accomplished by tilting.³⁸ In the crystal structure of HBC, this center-to-center lateral offset corresponds to nearly 40% of the molecular cross section.³⁰

It is remarkable that not only homeotropically aligned films could be produced here by simple solution processing but also that the tilting of the disks within the columns is suppressed. Thick films (microns) can be homeotropically aligned between glass slides starting from the melt,¹⁴ but random nucleation of the low-temperature phase occurs on further cooling, producing a polycrystalline sample. In the solution processed films here, it is likely that a tightly packed face-on monolayer is first formed, typically exploited for scanning tunneling microscopy measurements of HBC's at solution-solid interfaces. This layer serves to nucleate vertical growth of columns, corresponding to the melt process of homeotropic growth. A similar growth process from the gas phase was proposed in UHV deposited films of HBC (1a).¹⁵ The irreversible spectral changes observed here are probably not due to a phase transition similar to that observed in the bulk because the disks remain parallel to the surface at all temperatures, but instead to an increased perfection of the columns. In the as-prepared films, the disks may instead be regularly offset relative to the column axis, as was also proposed for the above-mentioned UHV deposited films.

B. $\text{C}_{132}\text{-C}_{16,4}$

The strong π - π interaction between individual molecular systems within stacks is one of the major forces that governs the formation of columnar structures. Molecules with an extended aromatic core, such as 2b, can be expected to exhibit a strong tendency for columnar packing. Figure 6 displays

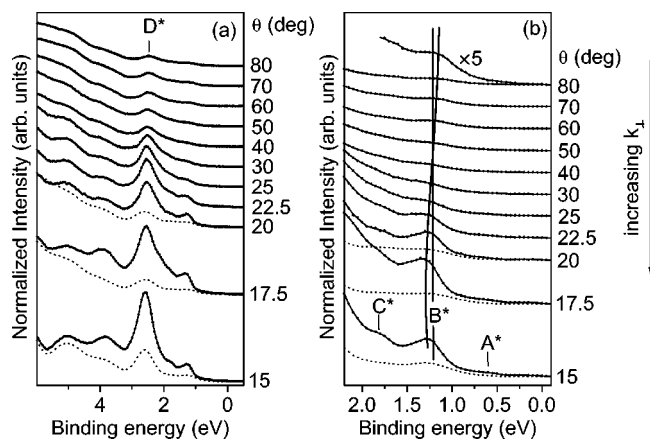


FIG. 6. ARUPS spectra of the $\text{C}_{132}\text{-C}_{16,4}$ (2b) films before (dotted line) and after heating (full line, circles) of the solution processed films in a wider (a) and narrower (b) energy range. Additionally, the shift of peak B^* with θ in the annealed films is indicated by a thick full line. Uppermost spectra in (b): those at $\theta = 80$ deg magnified by a factor of 10.

the angle-dependent valence-band spectra of $\text{C}_{132}\text{-C}_{16,4}$ films. It is intriguing that even the spectra of films of such large molecules, bearing 66 occupied π -electronic levels, are structured. It exhibits peaks at 0.60 (labeled A^*) and 1.30 eV (labeled B^*), a shoulder at about 1.80 eV (labeled C^*), a relatively broad and intense feature centered at 2.60 eV (labeled D^*), as well as peaks at about 3.8 and 5.1 eV. For this larger molecule more dramatic changes occur upon heating above 120–130 $^\circ\text{C}$, than were observed for 1c. For the heated films, kept at 140 $^\circ\text{C}$, the angular dependence of the spectra resembles that of the smaller 1c. As shown in Fig. 4(a) feature B^* disappears for θ higher than 30 deg, again indicating an orientation of the individual molecules parallel to the substrate surface, in the form of a one-dimensional stacking. As for the 1c films, the angular dependence of B^* is different and more pronounced than that of the dominant peak D^* shown in Fig. 4(b), which contains a larger density of π levels. For the as-prepared films of 2b, on the other hand, the spectra in Fig. 6 show a less-pronounced angular dependence and lower π intensity, suggesting a lack of one-dimensional arrangement in stacks normal to the substrate surface. Likewise, no thermal transition could be detected in the bulk material by differential scanning calorimetry.¹⁷ Wide-angle x-ray-scattering spectra obtained from oriented fibers reveal an increase in intracolumnar order upon annealing above 100 $^\circ\text{C}$;¹⁷ the reflex corresponding to the disk-disk stacking distance (~ 3.5 Å) sharpens and increases in relative intensity.

The electronic structure of the $\text{C}_{132}\text{-C}_{16,4}$ columnar stacks can be rationalized as follows: The broadening in the in-plane wave number, of $\Delta k_{\parallel} \sim 0.3 \text{ \AA}^{-1}$, is about 1/6 of the size of the graphene Brillouin zone. As expected, for a molecule with about double the diameter of HBC, the smearing of the in-plane quasimomentum k_{\parallel} is less pronounced. Compared to HBC, this leads to a decrease of about 10 deg of the angles at which strong π -electron emission is observed. As for the HBC derivative, the individual spectral features dis-

perse with θ (and thus k_{\perp}). Interestingly, the energy position of peak B^* turns back towards lower binding energy at an angle $\theta=17.5$ deg which might be related to the fact that the end of a Brillouin zone (not necessarily the first one) is reached. The energy shift of B^* between 17.5 deg and 70 deg amounts to about 0.22 ± 0.05 eV, which suggests a bandwidth W of this magnitude. However, due to the high number of electronic π levels involved, this interpretation is not unambiguous. As expected, the IP of the films of the larger molecule 2b (4.8 eV) is smaller than that of the 1c films (5.5 eV). In both cases, the IP changes only marginally upon heating.

IV. CONCLUSIONS

In conclusion, the investigated substituted PAH's are prone to self-assemble in ordered supramolecular architectures at surfaces. Solution processed nanometer thick films on solid substrates exhibit columnar order on a macroscopic scale which is improved upon heating to moderate temperatures. Supramolecular organization is considered to be driven by a strong π - π interaction between the aromatic cores. In multilayer films, the growth of the PAH's into columnar arrangements on the MoS_2 [0001] surface is likely to be substrate induced, initiated by the flat orientation of the molecules in the first layers. Unlike for thicker films, the columnar axis remains normal to the substrate throughout the multilayer. A broader view of homeotropic columnar growth is now available, where proper conditions allow growth from a ground floor, most likely a face-on monolayer of disks formed either in the melt, by UHV deposition, or now by solution processing. These molecular films exhibit interesting, highly anisotropic electronic properties. The intermolecular HOMO π -band dispersion in columnar HBC- $\text{C}_{8,2}$ films could be measured to be at least 0.15 ± 0.05 eV. The

individual π states are extended and form bands along the stacks, while there is quantization of the electronic states in the directions perpendicular to the axis. The observation of an initial-state smearing of k_{\parallel} suggests that the components of the in-plane quasimomentum k_x and k_y of the individual electronic states do not correspond exactly to those one would expect for a wave function in an infinitely extended graphene lattice. In this respect, these columns only partially constitute "one-dimensional graphite." Considering their high charge mobilities and the possibility of processing from solution these highly ordered, nanostructured films may certainly be expected to be of importance for future organic-electronic applications.

ACKNOWLEDGMENTS

The authors thank J. Sadowski (Chalmers University, Sweden), T. Balasubramanian (MAX-Lab), M. Tschaplyguine and G. Öhrwall (both Uppsala University, Sweden), M. Keil (Obducat A.B., Malmö, Sweden), C. Süß and R. Murdey (both Linköping University, Sweden), and the MAX-Lab user support group for help and discussions. M.P.d.J. was supported by the Center for Advanced Molecular Materials, CAMM, funded by the Swedish Foundation for Strategic Research (SSF), X.C. by a Marie-Curie Contract No. HPMF-CT-2000-00646, and W.O. by the European Community Research Training Network LAMINATE (Project No. 00135). Work in Linköping, Berlin and Mainz was supported by the EU-Growth project MAC-MES (Project No. GRD2-2000-30242). Otherwise, molecular and polymer research in Linköping was supported by the Swedish Science Research Council (VR), that in Mainz by the "Zentrum für multifunktionelle Werkstoffe und miniaturisierte Funktionseinheiten" (Grant No. BMBF 03N 6500).

*Email address: raifr@ifm.liu.se

[†]Present address: University of Kentucky, Department of Chemistry, Lexington, Kentucky 40506-0055.

[‡]Present address: Istituto per la Sintesi Organica e la Fotoreattività, Consiglio Nazionale delle Ricerche, 40129 Bologna, Italy.

¹A.M. van de Craats, J.M. Warman, A. Fechtenkötter, J.D. Brand, M.A. Harbison, and K. Müllen, *Adv. Mater. (Weinheim, Ger.)* **11**, 1469 (1999).

²A.M. van de Craats and J.M. Warman, *Adv. Mater. (Weinheim, Ger.)* **13**, 130 (2001).

³L. Schmidt-Mende, A. Fechtenkötter, K. Müllen, E. Moons, R.H. Friend, and J.D. MacKenzie, *Science* **293**, 1119 (2001).

⁴H. Sirringhaus, R.J. Wilson, R.H. Friend, M. Inbasekaran, W. Wu, E.P. Woo, M. Grell, and D.D.C. Bradley, *Appl. Phys. Lett.* **77**, 406 (2000).

⁵M. Paulsson and S. Stafström, *J. Phys.: Condens. Matter* **12**, 9433 (2000).

⁶C.-Y. Liu and A.J. Bard, *Nature (London)* **418**, 162 (2002).

⁷A. Tracz, J.K. Jeszka, M.D. Watson, W. Pisula, K. Müllen, and T. Pakula, *J. Am. Chem. Soc.* **125**, 1682 (2003).

⁸M.S. Dresselhaus, G. Dresselhaus, and P.C. Eklund, *Science of Fullerenes and Carbon Nanotubes* (Academic Press, San Diego, 1996).

⁹P. Samorí, N. Severin, C.D. Simpson, K. Müllen, and J.P. Rabe, *J. Am. Chem. Soc.* **124**, 9454 (2002).

¹⁰A. Stabel, P. Herwig, K. Müllen, and J.P. Rabe, *Angew. Chem., Int. Ed. Engl.* **34**, 1609 (1995).

¹¹P. Samorí, M. Keil, R. Friedlein, J. Birgerson, J.D. Brand, K. Müllen, W.R. Salaneck, and J.P. Rabe, *J. Phys. Chem. B* **105**, 11 114 (2001).

¹²Q.H. Wang, A.A. Setlur, J.M. Lauerhaas, J.Y. Dai, E.W. Seelig, and R.P.H. Chang, *Appl. Phys. Lett.* **72**, 2912 (1998).

¹³C.-Y. Liu, A. Fechtenkötter, M.D. Watson, K. Müllen, and A.J. Bard, *Chem. Mater.* **15**, 124 (2003).

¹⁴H.T. Jung, S.O. Kim, Y.K. Ko, D.K. Yoon, S.D. Hudson, V. Percec, M.N. Holerca, W.D. Cho, and P.E. Mosier, *Macromolecules* **35**, 3717 (2002).

¹⁵P. Ruffieux, O. Gröning, M. Biemann, C. Simpson, K. Müllen, L. Schlapbach, and P. Gröning, *Phys. Rev. B* **66**, 073409 (2002).

¹⁶A. Fechtenkötter, N. Tchebotareva, M. Watson, and K. Müllen, *Tetrahedron* **57**, 3769 (2001).

¹⁷C. D. Simpson, M. D. Watson, and K. Müllen (unpublished).

¹⁸M. Keil, P. Samorí, D.A. dos Santos, T. Kugler, S. Stafström, J.D. Brand, K. Müllen, J.L. Brédas, J.P. Rabe, and W.R. Salaneck, *J. Phys. Chem. B* **104**, 3967 (2000).

- ¹⁹M. Bässler, J.-O. Forsell, O. Björneholm, R. Feifel, M. Jurvansuu, S. Aksela, S. Sundin, S.L. Sorensen, R. Nyholm, A. Ausmees, and S. Svensson, *J. Electron Spectrosc. Relat. Phenom.* **101**, 953 (1999).
- ²⁰C.S. Fadley, in *Electron Spectroscopy: Theory, Techniques, and Applications*, edited by C.R. Brundle and A. D. Baker (Academic, London, 1978).
- ²¹D.T. Clark, M.M. Abu-Shbak, and W.J. Brennan, *J. Electron Spectrosc. Relat. Phenom.* **28**, 11 (1982).
- ²²H. Proehl, M. Toerker, F. Sellam, T. Fritz, K. Leo, C. Simpson, and K. Müllen, *Phys. Rev. B* **63**, 205409 (2001).
- ²³A.R. Law, J.J. Barry, and H.P. Hughes, *Phys. Rev. B* **28**, 5332 (1983).
- ²⁴A.R. Law, M.T. Johnson, and H.P. Hughes, *Phys. Rev. B* **34**, 4289 (1986).
- ²⁵P. Yannoulis, E.E. Koch, and M. Lähdeniemi, *Surf. Sci.* **192**, 299 (1987).
- ²⁶N. Ueno, A. Kitamura, K.K. Okudaira, T. Miyamae, Y. Harada, S. Hasegawa, H. Ishii, H. Inokuchi, T. Fujikawa, T. Miyazaki, and K. Seki, *J. Chem. Phys.* **107**, 2079 (1997).
- ²⁷F. Zwick, D. Jérôme, G. Margaritondo, M. Onellion, J. Voit, and M. Grioni, *Phys. Rev. Lett.* **81**, 2974 (1998).
- ²⁸K.K. Okudaira, S. Hasegawa, H. Ishii, K. Seki, Y. Harada, and N. Ueno, *J. Appl. Phys.* **85**, 6453 (1999).
- ²⁹W.D. Grobman, *Phys. Rev. B* **17**, 4573 (1978).
- ³⁰R. Goddard, M.W. Haenel, W.C. Herndon, C. Krüger, and M. Zander, *J. Am. Chem. Soc.* **112**, 5525 (1990).
- ³¹For substantially tilted molecules (of more than ~ 20 deg), one would expect two maxima as a function of θ to occur.
- ³²S. Hüfner, *Photoelectron Spectroscopy* (Springer-Verlag, Berlin, 1995).
- ³³S. Narioka, H. Ishii, K. Edamatsu, K. Kamiya, S. Hasegawa, T. Ohta, N. Ueno, and K. Seki, *Phys. Rev. B* **52**, 2362 (1995).
- ³⁴S. Hasegawa, T. Mori, K. Imaeda, S. Tanaka, Y. Yamashita, H. Inokuchi, H. Fujimoto, K. Seki, and N. Ueno, *J. Chem. Soc.* **100**, 6969 (1994).
- ³⁵J. Cornil, V. Lemaire, J.-P. Calbert, and J.L. Brédas, *Adv. Mater. (Weinheim, Ger.)* **13**, 1053 (2002).
- ³⁶J.L. Brédas, J.P. Calbert, D.A. da Silva Filho, and J. Cornil, *Proc. Natl. Acad. Sci. U.S.A.* **99**, 5804 (2002).
- ³⁷O. Bunk, M.M. Nielsen, T.I. Sølling, A.M. van de Craats, and N.J. Stutzmann, *J. Am. Chem. Soc.* **125**, 2252 (2003).
- ³⁸C.A. Hunter, K.R. Lawson, J. Perkins, and C.J. Urch, *J. Chem. Soc., Perkin Trans. 2* **2001**, 651; C.A. Hunter and J.K.M. Sanders, *J. Am. Chem. Soc.* **112**, 5525 (1990).